

Mid-Infrared NGST Studies of Protostars

M. Barsony^{1,2}

Harvey Mudd College, Claremont CA 91711 and

Jet Propulsion Laboratory, MS 169-327, Pasadena, CA 91109

B. Whitney

Space Science Institute, Boulder, CO 80303

Abstract. Given a mid-infrared (MIR) Next Generation Space Telescope (NGST) instrument working out to $30\ \mu\text{m}$, our understanding of the star-formation process would be revolutionized. We stress that the MIR observations of protostars modeled here would be impossible to obtain from any other platform. Detailed Monte Carlo radiative transfer calculations of protostellar envelopes were run at three MIR and three submillimeter wavelengths to demonstrate the complementarity of information that could be gleaned by combining NGST and Atacama Large Millimeter Array (ALMA) data.

1. Introduction

The result of research since the successful Infrared Astronomical Satellite (IRAS) mission and the commissioning of large-aperture, ground-based submillimeter telescopes such as the James Clerk Maxwell Telescope (JCMT) has led to our current understanding of the four stages of star-formation (Adams, Lada, & Shu 1987, Chandler et al. 1990, Lada 1991, Barsony 1994):

- **Class 0 Sources:** These objects are in the youngest observable protostellar stage which lasts just a few $\times 10^4$ years (André, Ward-Thompson, & Barsony 1993). Dynamic infall is occurring onto a central hydrostatic core which contains less mass than its surrounding dense, extended infall envelope (André & Montmerle 1994). Class 0 sources are characterized by powerful bipolar molecular outflows (Bontemps et al. 1996, Wolf-Chase et al. 1998) and spectral energy distributions resembling a modified, single temperature, cold ($T \leq 30\text{K}$) blackbody (Barsony 1994).
- **Class I Sources:** In this stage, which lasts a few $\times 10^5$ yr (Kenyon et al. 1990), the central object has attained $\geq 90\%$ of its final Zero Age

¹NSF POWRE Visiting Professor

²CAREER Award Recipient

Main Sequence (ZAMS) mass. The nascent star is now surrounded by an accretion disk and a remnant infall envelope which has been excavated by the outflow to contain bipolar cavities (Padgett et al. 1999; Velusamy & Langer 1998). The majority (60%–80%) of these sources are still driving bipolar outflows, but these are ten times less powerful than those observed in the Class 0 stage. The SED's of Class I sources are broader than a blackbody distribution, rise from $2\ \mu\text{m}$ – $10\ \mu\text{m}$, and peak in the far-infrared (e.g., Wilking, Lada, & Young 1989, Ladd et al. 1991).

- **Class II Sources:** This stage lasts of order a few $\times 10^6$ yr (Hillenbrand 1998, White et al. 1999) and is characterized by an emission-line star, (T-Tauri star), surrounded by a substantial disk (e.g., McCaughrean & O'Dell 1996; Beckwith et al. 1990, Koerner & Sargent 1995, Guilloteau & Dutrey 1998). The infall envelope and outflow have both largely disappeared by this stage. The SED's of Class II objects are broader than a blackbody distribution, peaking around $2\ \mu\text{m}$ – $3\ \mu\text{m}$, falling from $2\ \mu\text{m}$ – $10\ \mu\text{m}$ (Rucinski 1985).
- **Class III Sources:** This is the final pre-main-sequence stage, lasting 10^6 – 10^7 yr (Walter et al. 1988). From the perspective of planet formation, this is the most exciting stage to study, since the typical $0.1\ M_{\odot}$ of disk material present in the Class II stage has evolved to a disk mass $\leq 0.001\ M_{\odot}$, deduced from the lack of detectable millimeter continuum flux in such sources (André & Montmerle 1994). Presumably, most of the particulate material has agglomerated into planetesimals or even planets at this stage in the mostly gaseous disk. The only direct way to detect the warm gas in these disks is through the $28\ \mu\text{m}$ and $17\ \mu\text{m}$ emission lines of H_2 , as has recently been done by ISO in the case of a source bright enough for detection, the Class II binary system GG Tau (Thi et al. 1999). The SED's of Class III sources resemble reddened stellar blackbodies.

To date, all 45 known Class 0 protostars within 500 pc of the Sun remain either undetected in the MIR, or, if detected by ISOCAM (with $6''$ pixels), they appear as weak (mJy level) point sources (André, Ward-Thompson, & Barsony 1999). NGST's unparalleled combination of sensitivity and angular resolution will be able to reveal, for the first time, the otherwise obscured, warm (a few $\times 100$ K) inner dust structures closest to the central accreting protostar.

2. Models

To demonstrate what could, in principle, be learned from MIR NGST imaging of protostars, we ran a 2-D Monte Carlo radiative transfer code (Whitney & Hartmann 1993) to simulate the appearance of a Class 0 object at various wavelengths. The code has been modified to include thermal emission from the star, disk and envelope, assuming the envelope temperature follows a $T \propto r^{-0.4}$ power law (Wolfire & Cassinelli 1986). For the figures shown below, a nearly edge-on orientation ($i = 80^\circ$) was assumed for the 10 AU radius accretion disk, buried in infalling envelope of 3000 AU radius, with a bipolar cavity of 10° opening angle.

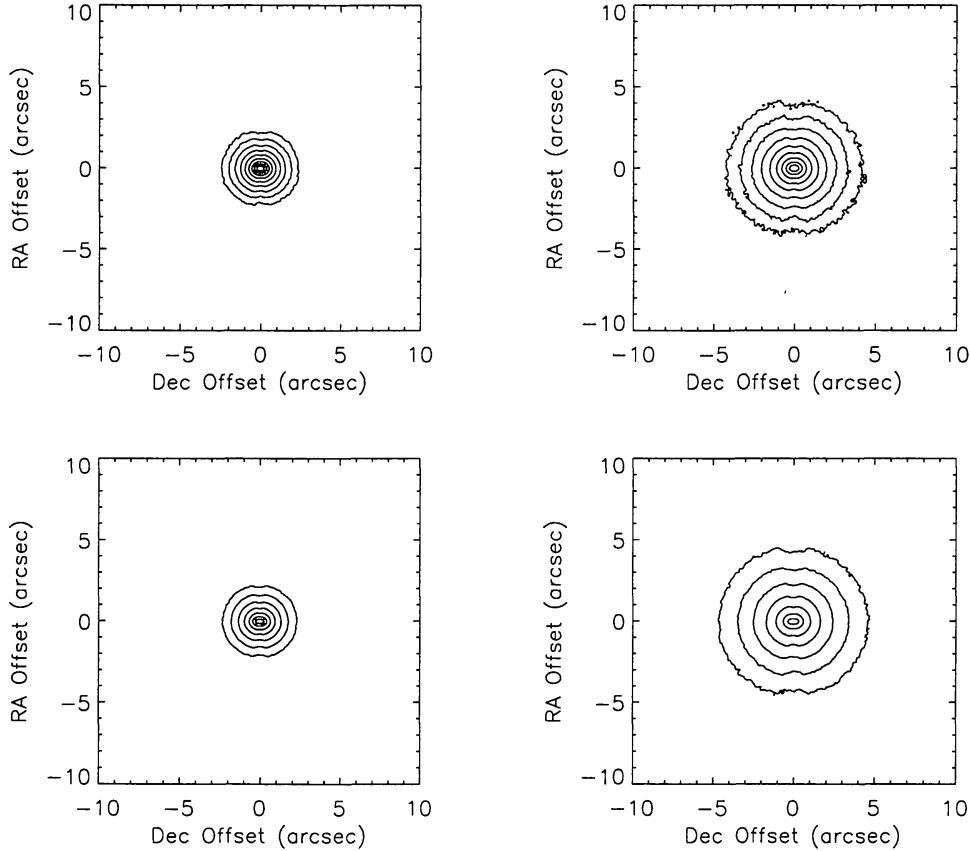


Figure 1. Model images of a Class 0 protostar at $20\ \mu\text{m}$ (left panels), and $28\ \mu\text{m}$ (right panels). Top: Envelope structure is rotationally flattened (TSC) with a centrifugal radius of $r_c = 10\ \text{AU}$; the density falls off as $n(r) \propto r^{-3/2}$ beyond r_c ; the total $A_V = 496$. Bottom: The envelope density follows $n(r) \propto r^{-1/2}$ at all radii; the total $A_V = 467$. For all panels, the minimum contour levels are $0.01\ \text{mJy/pixel}$ for a system luminosity of $1\ L_\odot$ and distance of $125\ \text{pc}$. Each contour interval increases by 1 magnitude. The closely spaced contours in the top panels reflect the steeper density law.

The envelope density structure is a crucial quantity capable of distinguishing amongst competing star-formation theories. The standard model of an envelope in free-fall collapse, modified by rotation, gives a density that goes as $n(r) \propto r^{-1/2}$ in the inner regions, within a centrifugal radius r_c , and $n(r) \propto r^{-3/2}$ at radii greater than r_c (Terebey, Shu, & Cassen 1984; TSC). In the youngest, or Class 0 sources, r_c is expected to be small ($< 10\ \text{AU}$, or $0.08''$ at a distance to the nearest star forming region) and the standard theory therefore predicts $n(r) \propto r^{-3/2}$ over most of the observable envelope. Such a model is presented in the top panels of Figure 1.

Model fits to the SEDs of Class 0 sources, however, seem to require that the density follow a $r^{-1/2}$ power law (André et al. 1993). Theories of binary formation (Bonnell, Bate, & Price 1996, Bate, Bonnell, & Price 1995) as well

as hydrodynamical simulations of infall from non-ideal cloud cores (Foster & Chevalier 1993, Galli & Shu 1993) also predict a flatter density law than the “standard” (TSC) model. The bottom panels of Figure 1 show model images for a shallower, $n(r) \propto r^{-1/2}$ density distribution. This envelope has a similar A_V to the standard TSC model at this particular viewing angle, but the A_V 's remain high over a wider range of inclinations. Thus, this flat-density envelope has more mass, more extinction at short wavelengths over a larger range in viewing angle, and more emission at long wavelengths. Images were also computed at $10\mu\text{m}$ (not shown) where the TSC model gives an integrated flux of 0.4 mJy and the flat-density model gives a flux nine orders of magnitude fainter. That is, the flat-density model produces a much redder SED. The MIR fluxes are sensitive to source inclination, allowing further constraints on source characteristics.

The comparison of MIR images from NGST with quantitative models of the MIR appearance of Class 0 infalling envelopes will sufficiently narrow the range of allowable envelope density laws and thus distinguish between current theories of star formation. To further constrain envelope structures requires fitting the entire SED from MIR through millimeter wavelengths. In addition, the accretion disk size for Class 0 protostars can be independently determined with ALMA. Figure 2 shows how the sub-millimeter images can also distinguish between envelope geometries, though they are not as sensitive to inclination as the MIR. Thus, both wavelength regimes are highly complementary.

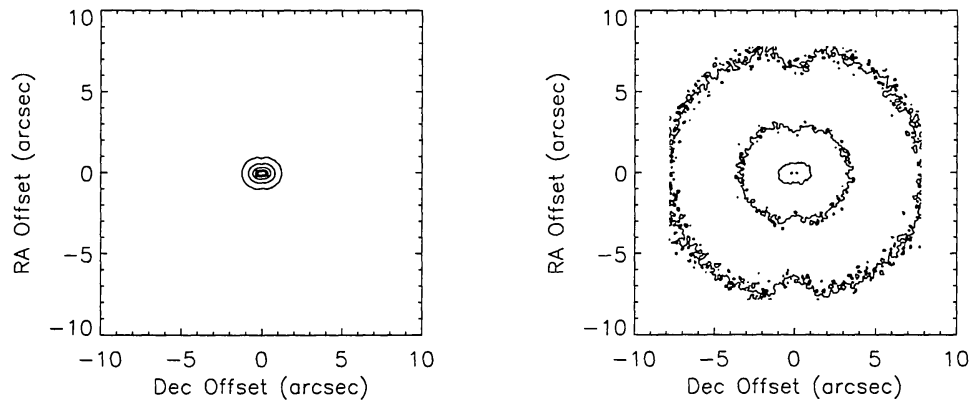


Figure 2. Model images at $350\ \mu\text{m}$. On the left is the standard TSC envelope (as in top of Figure 1). On the right is the flattened-density envelope (as in bottom of Figure 1). Both are plotted with the same minimum contour of 5 mJy. Contour spacing is 0.5 magnitudes. The envelope emission traces the density distribution, and also delineates the inner disk region.

References

Adams, F.C. Lada, C.J., & Shu, F.H. 1987, *ApJ*, 312, 788

- André, P., Ward-Thompson, D., & Barsony, M. 1999, in *Protostars & Planets IV*, eds. V. Mannings, A.P. Boss, & S.S. Russell (Tucson: Univ. of Arizona Press)
- André, P., Ward-Thompson, D., & Barsony, M. 1993, *ApJ*, 406, 122
- André, P. & Montmerle, T. 1994, *ApJ*, 420, 837
- Barsony, M. 1994, in *Clouds, Cores, & Low Mass Stars*, eds. D. P. Clemens & R. Barvainis, ASP Conf. Ser. 65, 197
- Bate, M.R., Bonnell, I.A., & Price, N.M. 1995, *MNRAS*, 277, 362
- Beckwith, S.V.W., Sargent, A.I., Chini, R.S. & Güsten, R. 1990, *AJ*, 99, 924
- Bonnell, I.A., Bate, M.R., & Price, N.M. 1996, *MNRAS*, 279, 121
- Bontemps, S., André, P., Terebey, S., & Cabrit, S. 1996, *A&A*, 311, 858
- Chandler, C.J., Gear, W.K., Sandell, G., Hayashi, S., Duncan, W.D., & Griffin, M.J. 1990, *MNRAS*, 243, 330
- Foster, P., & Chevalier, R.A. 1993, *ApJ*, 416, 303
- Galli, D., & Shu, F.H. 1993, *ApJ*, 417, 220
- Guilloteau, S. & Dutrey, A. 1998, *A&A*, 339, 467
- Hillenbrand, L.A., Strom, S.E., Calvet, N., Merrill, K.M., Gatley, I., Makidon, R.B., Meyer, M.R., & Skrutskie, M.F. 1998, *AJ*, 116, 1816
- Kenyon, S.J., Hartmann, L.W., Strom, K.M., & Strom, S.E. 1990, *AJ*, 99, 869
- Koerner, D.W. & Sargent, A.I. 1995, *AJ*, 109, 2138
- Lada, C.J. 1991, in *The Physics of Star Formation and Early Stellar Evolution*, eds., C.J. Lada & N.D. Kylafis, Dordrecht: Reidel, 329
- Ladd, E.F., Adams, F.C., Casey, S., Davidson, J.A., Fuller, G.A., Harper, D.A., Myers, P.C., & Padman, R. 1991, *ApJ*, 366, 203
- McCaughrean, M.J. & O'Dell, R.C. 1991, *AJ*, 111, 1977
- Padgett, D.L., Brandner, W., Stapelfeldt, K.R., Strom, S.E., Terebey, S. & Koerner, D. 1999, *AJ*, 117, 1490
- Rucinski, S.M. 1985, *AJ*, 90, 2321
- Terebey, S., Shu, F.H., & Cassen, P. 1984 (TSC), *ApJ*, 286, 529
- Thi, W.F., van Dishoeck, E.F., Blake, G.A., Van Zadelhoff, G. J., Hogerheijde, M.R. 1999, *ApJ*, 521, L63
- Velusamy, T. & Langer, W.D. 1998, *Nature*, 392, 685
- Walter, F.M., Brown, A., Mathieu, R.D., Myers, P.C., & Vrba, F.J. 1988, *AJ* 96 297
- White, R.J., Ghez, A.M., Reid, I.N., & Schultz, G. 1999, *ApJ*, 520, 811
- Whitney, B.A., & Hartmann, L. 1993, *ApJ*, 402, 605
- Wilking, B.A., Lada, C.J., & Young, E.F. 1989, *ApJ*, 340, 923
- Wolf-Chase, G.A., Barsony, M., Wootten, A.H., Ward-Thompson, D., Lowrance, P.J., Kastner, J.H., & McMullin, J.P. 1998, *ApJ*, 501 L198
- Wolfire, M.G., & Cassinelli, J.P. 1986, *ApJ*, 310, 207